

Single-Photon Advantage in Quantum Cryptography Beyond QKD

Daniel A. Vajner,^{1,*} Koray Kaymazlar,^{1,*} Fenja Drauschke,^{2,*}
Lucas Rickert,¹ Martin v. Helversen,¹ Hanqing Liu,^{3,4} Shulun Li,^{3,4}
Haiqiao Ni,^{3,4} Zhichuan Niu,^{3,4} Anna Pappa,² and Tobias Heindel^{1,†}

¹*Institute of Solid State Physics, Technical University of Berlin, 10623 Berlin, Germany*

²*Electrical Engineering and Computer Science Department,
Technical University of Berlin, 10623 Berlin, Germany*

³*Key Laboratory of Optoelectronic Materials and Devices, Institute of
Semiconductors, Chinese Academy of Sciences, Beijing, 100083, China*

⁴*Center of Materials Science and Optoelectronics Engineering,
University of Chinese Academy of Sciences, Beijing, 100049, China*

Abstract

In quantum cryptography, fundamental laws of quantum physics are exploited to enhance the security of cryptographic tasks. Quantum key distribution is by far the most studied protocol to date, enabling the establishment of a secret key between trusted parties. However, there exist many practical use-cases in communication networks, which also involve parties in distrustful settings. The most fundamental quantum cryptographic building block in such a distrustful setting is quantum coin flipping, which provides an advantage compared to its classical equivalent. So far, few experimental studies on quantum coin flipping have been reported, all of which used probabilistic quantum light sources facing fundamental limitations. Here, we experimentally implement a quantum strong coin flipping protocol using single-photon states and demonstrate an advantage compared to both classical realizations and implementations using faint laser pulses. We achieve this by employing a state-of-the-art deterministic single-photon source based on the Purcell-enhanced emission of a semiconductor quantum dot in combination with fast polarization-state encoding with a quantum bit error ratio below 3%, required for the successful execution of the protocol. The reduced multi-photon emission yields a smaller bias of the coin flipping protocol compared to an attenuated laser implementation, both in simulations and in the experiment. By demonstrating a single-photon quantum advantage in a cryptographic primitive beyond QKD, our work represents a major advance towards the implementation of complex cryptographic tasks in a future quantum internet.

I. INTRODUCTION

The functionality of today's communication networks relies on diverse, sensitive and complex tasks which, nevertheless, can be built from a set of basic cryptographic building blocks, or primitives. While the security of classical cryptographic implementations relies on assumptions regarding e.g. the computational complexity, it is known that laws of quantum physics can be exploited to enhance the security in communication [2, 3, 30]. To date, quantum key distribution (QKD) is by far the most studied quantum cryptographic primitive, enabling unconditional security in the communication between authenticated, trusted

* These authors contributed equally

† tobias.heindel@tu-berlin.de

parties. Despite its importance and success, QKD is fundamentally limited in its usefulness, as it cannot be used for more complex cryptographic tasks. Many practical use-cases involve two or more parties who do not know or trust each other, but still want to interact (e.g. for doing business) [9].

An important example of a cryptographic primitive between two distrustful parties is coin flipping (CF), where two parties toss a coin to choose between two alternatives in the least biased way. Due to the importance of this primitive, M. Blum introduced the idea of 'coin flipping by telephone' already in 1983, in which two spatially separated parties do not necessarily trust each other but still wish to ensure that the outcome of the coin flip is unbiased [6]. As classical coin-flipping protocols rely on the computational complexity of one-way functions, they can always be broken with sufficient computational power under standard non-relativistic assumptions [10].

This is not the case in the quantum version of coin flipping protocols [1], although a finite bias remains [17, 18]. Interestingly, the first quantum coin flipping protocol has been proposed in the very same seminal work by C.H. Bennett and G. Brassard in 1984 [2]. While this and many other protocols seemed impractical, more recent proposals accounted for device imperfections and channel loss, unavoidable in practical scenarios [4, 23]. Experimental implementations of quantum coin flipping reported to date used attenuated lasers, i.e. weak coherent pulses (WCPs) [22, 24], sources based on spontaneous parametric down conversion (SPDC) exploiting entanglement [5, 20], or heralded single photon states [21], which are fundamentally limited in their efficiency. However, as demonstrated in our work, deterministic quantum light sources providing single photons on-demand, can provide an advantage for implementations of cryptographic primitives beyond QKD.

In this work we experimentally implement a quantum strong coin flipping protocol using an on-demand sub-Poissonian light source and demonstrate its advantage over both classical and WCP-based implementations. To this end, we employ a state-of-the-art single-photon source based on a semiconductor quantum dot deterministically integrated into a high-Purcell micro-cavity in combination with fast dynamic polarization-state encoding with a sufficiently low quantum bit error ratio, required for the successful execution of this type of protocol. Based on a thorough theoretical analysis, we optimize the protocol parameters and experimentally achieve quantum coin flipping rates on the order of ≈ 1 kbit/s in back-to-back configuration. We observe cheating probabilities lower than what is possible

in the equivalent classical coin flipping protocol, both in simulations and in the experiment. Moreover, we conducted QSCF experiments under variable attenuation inside the quantum channel and study its impact on the quantum advantage. Our work represents an important step forward in exploiting quantum advantages in realistic settings for applications in the future quantum internet.

II. RESULTS

A. The quantum coin flipping protocol

In the context of quantum coin flipping, similar to classical coin flipping, two protocol families, known as quantum strong coin flipping (QSCF) and quantum weak coin flipping (QWCF), are distinguished according to the goals of the two parties. While in QWCF both parties favor a certain outcome (e.g. Alice wants 0 and Bob wants 1, and they are aware of the other party's preference), both parties want a random, unbiased result in QSCF. Hence, cheating in QWCF must be considered in one direction only, while both directions are important in QSCF, resulting in more protocol constraints for the latter type. The security of a coin flipping protocol is measured by the bias ϵ , that quantifies how much the cheating probability differs from the case of random guessing with probability $1/2$. The minimum theoretically achievable bias for a QSCF protocol was shown by Kitaev to be $\epsilon \leq \frac{1}{2}(\sqrt{2} - 1) \approx 0.21$ [16], which corresponds to a minimum cheating probability of 71%. On the other hand, QWCF protocols with arbitrarily small bias exist [19], which are, however, often based on assumptions difficult to achieve experimentally. More recently, a newly proposed QWCF protocol [7] reaching Kitaev's bias limit was also successfully implemented experimentally [21]. Note that a successful implementation of QSCF always trivially implies a QWCF version of the same bias, as the two parties can simply place bets on the outcome of the unbiased random bit.

The protocol chosen for the implementation in this work is one of the most established ones in the family of QSCF protocols and has been proposed in Ref. [4] and extended in Ref. [23]. Previously, this protocol was used to show an experimental quantum advantage using attenuated laser pulses [24]. In the following, we first introduce the QSCF protocol and discuss on the basis of simulations how single photons can be exploited to enhance its

quantum advantage, before we turn to the experimental implementation.

The main steps of the QSCF protocol from Ref. [23] implemented in this work are the following (cf. Figure 1)[24]:

1. In each step i of a K -step long protocol round, Alice prepares and sends pulse $i \in (1, K)$ to Bob, in a randomly chosen preparation basis $\alpha_i \in \{0, 1\}$ and encoding bit value $c_i \in \{0, 1\}$. The four possible states $|\phi_{\alpha_i, c_i}\rangle$ read:

$$\begin{aligned} |\phi_{\alpha_i, 0}\rangle &= \sqrt{a}|0\rangle + (-1)^{\alpha_i}\sqrt{1-a}|1\rangle \text{ and} \\ |\phi_{\alpha_i, 1}\rangle &= \sqrt{1-a}|0\rangle - (-1)^{\alpha_i}\sqrt{a}|1\rangle, \end{aligned} \quad (1)$$

with the real number $a \in (0.5, 1)$, used to fine-tune the initial states to optimize the protocol and ensure equal cheating probabilities of Alice and Bob.

2. Bob picks a random measurement basis β_i for each pulse. If Bob has not detected any of the K pulses, the protocol aborts, otherwise the first detection event is j .
3. Bob picks a random number b_j and sends it to Alice via a classical channel together with the index j .
4. Alice reveals her corresponding basis and bit value (α_j, c_j) to Bob.
5. Whenever the same basis was used ($\alpha_j = \beta_j$), Bob confirms whether he measured the same state $|\phi_{\alpha_j, c_j}\rangle$ or aborts if the states disagree.
6. If Bob has not aborted, the outcome of the coin flip is $c_j \oplus b_j$

The probability P_{AB} that this protocol aborts even if neither party has cheated depends on different protocol parameters such as the number K of pulses sent per coin flip, the transmission η_{Bob} of Bob's receiver module, the detection efficiency η_{Det} of Bob's detector, the detection error e , the mean number of photons per pulse μ and the photon statistics of the employed light source. The latter also crucially affects the protocol performance as discussed in the following. Phase-randomized weak coherent pulses follow a Poisson distribution, i.e. the probability p_n that a pulse contains n photons depends on the mean photon number μ according to $p_n = \frac{e^{-\mu}\mu^n}{n!}$. In contrast, the photon statistics of a deterministic single-photon source, as used in our implementation, is limited by experimental imperfections only. In this

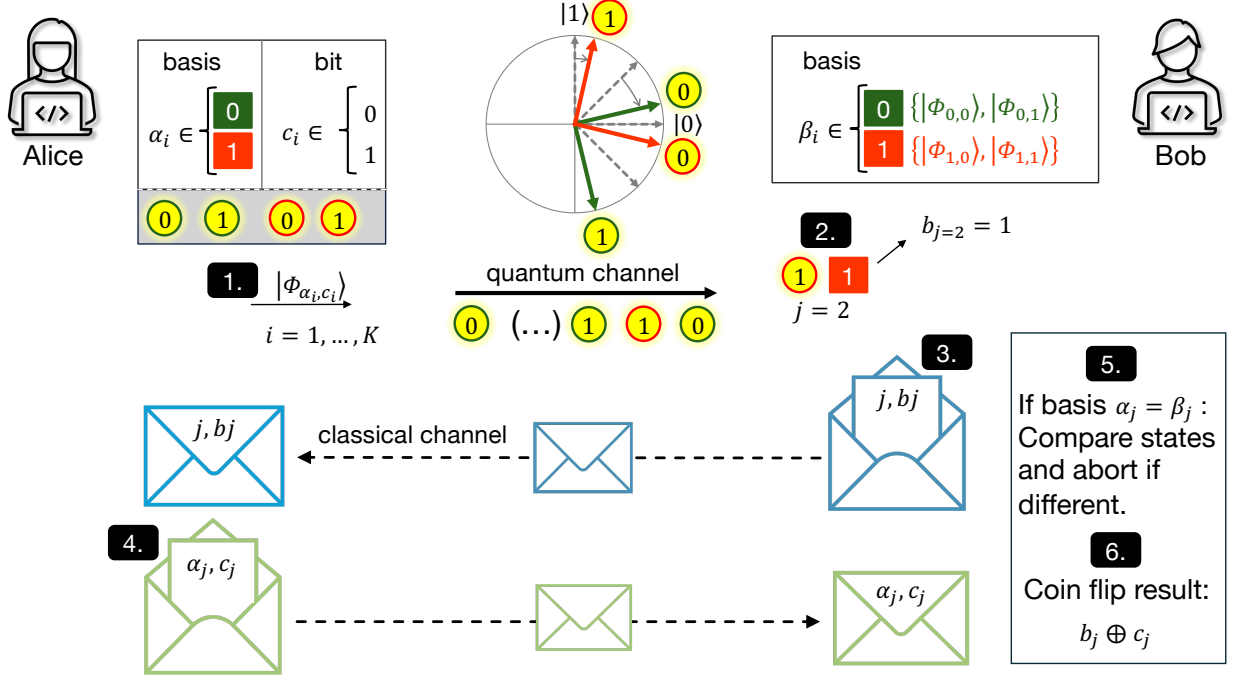


Figure 1. Schematic of the QSCF protocol implemented in this work: 1. Alice randomly prepares pulse number i of the K -long sequence in one out of four pre-optimized coin flipping states $|\phi_{\alpha_i, c_i}\rangle$ and sends them to Bob. The states are rotated relative to the standard BB84 states (dashed gray lines). 2. Bob projects the received pulses randomly into one of the same four states and calls the first detected event j . 3. Bob now sends a random number b_j and the pulse number j to Alice. 4. Alice returns her initial bit c_j and basis α_j for that pulse. 5. If Bob measures a different state for the same basis, he aborts. 6. If the protocol is not aborted the unbiased coin flip result is $c_j \oplus b_j$.

case, the amount of multi-photon contribution can be upper-bounded via the anti-bunching value $g^{(2)}(0)$ as [29]

$$p_1 \approx \mu, \quad p_2 \leq \frac{1}{2} \mu^2 g^{(2)}(0), \quad p_0 \approx 1 - p_1 - p_2. \quad (2)$$

B. Protocol Performance Simulation

Next, we simulate the performance of the QSCF protocol to evaluate the optimal parameters for our implementation. Accounting for the experimental conditions in our protocol implementation, the cheating probabilities can be calculated as a function of the protocol parameter a defining the tilt-angle in the four coin flipping states (cf., Eq. 1). Optimizing

the parameter a one can minimize the cheating probabilities under the fairness constraint for each parameter from the set $\{\mu, K, \vec{p}\}$. This optimization is performed for the parameters summarized in Table I corresponding to the experimental conditions realized in our implementation further below. Figure 2a shows the obtained optimized cheating probabilities as a function of the number of rounds K for a QSCF protocol implemented with weak coherent pulses (WCP, cf. blue line), a single photon source (SPS, cf. green line) and the equivalent classical protocol (black line). A quantum advantage is achieved when the QSCF cheating probability is smaller than in the classical protocol (blue shaded region). As the SPS implementation outperforms the WCP version over the full parameter range, at high K values only the SPS can achieve a quantum advantage (green shaded region).

An extended comparison between SPS and WCP implementation confirms that both provide a quantum advantage for realistic parameters, while the advantage is higher for the SPS. Figure 2b and c illustrates the difference between classical cheating probability and QSCF cheating probability, so that regions of positive values identify a quantum advantage. One finds that the reduced multi-photon contribution of the SPS-based implementation enables a quantum advantage for a larger range of parameters.

In this context, two aspects of QSCF are noteworthy compared to QKD: Firstly, the concept of decoy-states for mitigating multi-photon effects, as known from laser-based QKD [15], cannot be employed in the distrustful setting of coin flipping. Hence, all multi-photon

Parameter	Value
Detection module transmission η_{Bob}	0.5
Detector efficiency η_{Det}	0.85
QBER e	0.028
Anti-bunching value $g^{(2)}(0)$	0.03
Mean photon number μ	0.0013
Protocol rounds K	5×10^4
State parameter a	0.9
System clock rate R_0	80 MHz
Dark-count probability P_{dc}	4×10^{-7}

Table I. Parameters used in QSCF protocol simulations, matching the experimental conditions.

events increase the cheating possibilities for Bob. Secondly, achieving a quantum advantage in the QSCF protocol is more sensitive to bit errors. For our experimental parameters, QBERs below $\approx 4\%$ are required to achieve a quantum advantage, while BB84-QKD can tolerate up to 11% QBER and still asymptotically generate a secure key [12]. The reason is that in QKD errors can be mitigated during post-processing, while they reduce the equivalent classical cheating probability in QSCF due to an increased number of protocol aborts. Note that the employed cheating probability bound for Bob in the QSCF protocol is not tight and lower bounds might be found in the future which would increase the effective quantum advantage.

It should be noted that the same cheating probabilities and almost the same quantum advantage of the single-photon source could, in principle, be reproduced using a laser with a smaller mean photon number μ , as the likelihood of multi-photon events is proportional to μ^2 . However, a smaller μ would require higher K values leading to a lower rate of successful coin flips, as the maximum rate of unbiased coin flips is $R_{CF} = R_0/K \sim R_0 \cdot \mu$, where R_0 is the system clock-rate. Therefore, employing sub-Poissonian light sources in QSCF provides not only a reduced bias but also a better performance for the same bias.

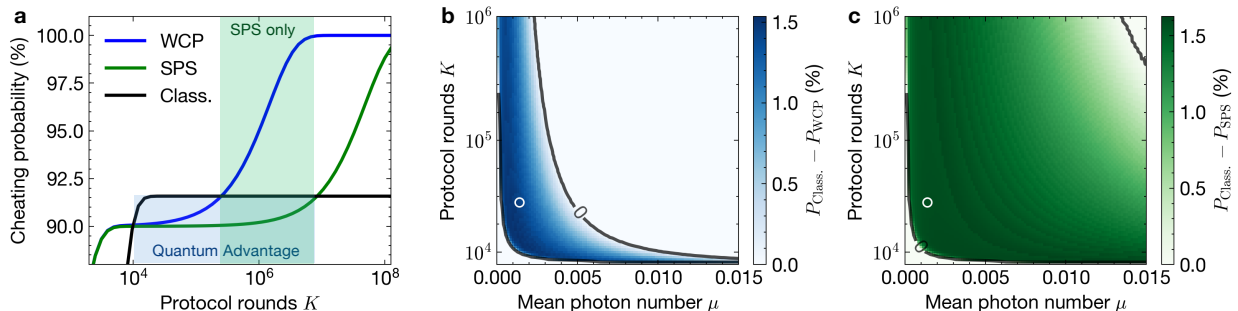


Figure 2. (a) Cheating probabilities for the QSCF protocol considered in this work as a function of the number of rounds K per coin flip for implementations using a single-photon source (SPS, green), weak coherent pulses (WCP, blue), and an equivalent classical implementation (Class., black) assuming $\mu = 0.0013$. (b) and (c) Reduction of cheating probability compared with classical protocol as a function of K and μ achievable in the QSCF protocol implemented with an attenuated laser and a sub-Poissonian light source ($g^{(2)}(0) = 0.03$), respectively. White circles mark the operating point of our experiment.

C. Experimental setup

To implement the QSCF protocol simulated above, we realized the experimental setup shown in Figure 3a. Below we first introduce the overall concept before discussing important experimental details. Alice uses a deterministic single-photon source to generate flying qubits at a clock-rate of $R_0 = 80$ MHz and dynamically switches randomly between the four different polarization-encoded QSCF states. Next, the polarization qubits propagate through a short free-space optical channel, including a variable attenuator for emulating channel loss. The single-photon pulses are detected by Bob using a passive basis choice 4-state polarization analyzer in combination with superconducting nanowire detectors and time-tagging electronics. Classical post-processing is performed via a classical data link. The execution of the QSCF protocol relies on two building blocks, namely the single-photon generation and the dynamic qubit encoding on Alice's side, as discussed in the following.

1. Flying qubit generation

The single-photon source comprises a single pre-selected semiconductor quantum dot emitting at a wavelength of 921 nm, deterministically integrated into a micro-cavity based on a hybrid circular Bragg grating (cf. inset in Figure 3a) to enhance the photon extraction efficiency and reduce the radiative lifetime to 50 ps via high Purcell enhancement. For details on the design, deterministic fabrication and in-depth quantum-optical characterization of this type of single-photon source we refer to Ref. [25] and [26], respectively. Choosing quasi-resonant (p-shell at 896 nm) optical excitation of the quantum emitter operated in a cryogenic environment (4 K) results in the emission spectrum in Figure 2b. Here, the predominant emission of a charged state used for our experiments in the following is identified. Performing a Hanbury-Brown and Twiss measurement after spectral filtering via a monochromator and coupling to a single-mode fiber confirms the single-photon nature of the emission with an uncorrected and integrated anti-bunching value of $g^{(2)}(0) = 0.03(1)$ (cf. Figure 3c). Furthermore, it is essential for the protocol implementation that the emitted photon states possess no coherence in the photon number basis, a necessary assumption in the treated cheating strategies, as recently discussed by Bozzio et al. [8]. This was confirmed for the excitation conditions used in the coin flipping implementation, by interfering sequen-

tially emitted single photons in a Mach-Zehnder-interferometer and varying their relative phase while monitoring the countrate after the interference. The absence of any oscillations confirms that no PNC is present (cf. Figure 3d, darker curves), thus, the analytical formalism based on Ref. [24] can be applied without the need for active phase-randomization. To make sure that the PNC measurement is performed correctly, we also excited the same QD resonantly with a pulse area of around 0.2π , yielding oscillations in the counts at the BS output, indicating the presence of PNC under resonant excitation (light curves).

2. *Dynamic polarization state encoding*

Dynamic state preparation on Alice’s side is performed using a fiber-coupled EOM controlled by a self-built arbitrary waveform generator based on field-programmable gate-array (FPGA) electronics, digital-to-analog converters (DAC) and an amplifier (Amp). The polarization encoded qubit states leaving the EOM are then rotated into the final protocol states via fiber polarization paddles just before entering the quantum channel. Figure 4a illustrates the desired qubit states and the corresponding polarization Stokes vector \vec{s} on the Poincaré sphere. Note that the voltage levels corresponding to the desired polarization states need to be carefully adjusted, due to the relatively small difference to the standard BB84 states. In the protocol implementation reported further below, the necessary random switching between the different states would usually result in time-dependent voltage level drifts in the control electronics before the EOM, which would in-turn increase the observed quantum bit errors. For this reason we employed a refined coding scheme, which builds on the idea of binary phase-keying or Manchester coding, to avoid drifts of the control electronics. The required doubling of the effective clock rate inside the AWG (from 80 to 160 MHz) makes the precise timing control more demanding, but effectively suppresses voltage level drifts in random state sequences, enabling low QBER levels with improved temporal stability. Figure 4b shows an exemplary random voltage level sequence used as input for the EOM in our protocol implementation, where the alternating voltage modulation was applied. This measurement confirms the correct adjustment of the voltage levels to the four target states for our implementation (full lines). Please note the small but crucial difference between the BB84 states (dashed gray lines), that one would apply in QKD experiments, and the QSCF states used in this work corresponding to $a = 0.9$, which are not equidistant anymore and

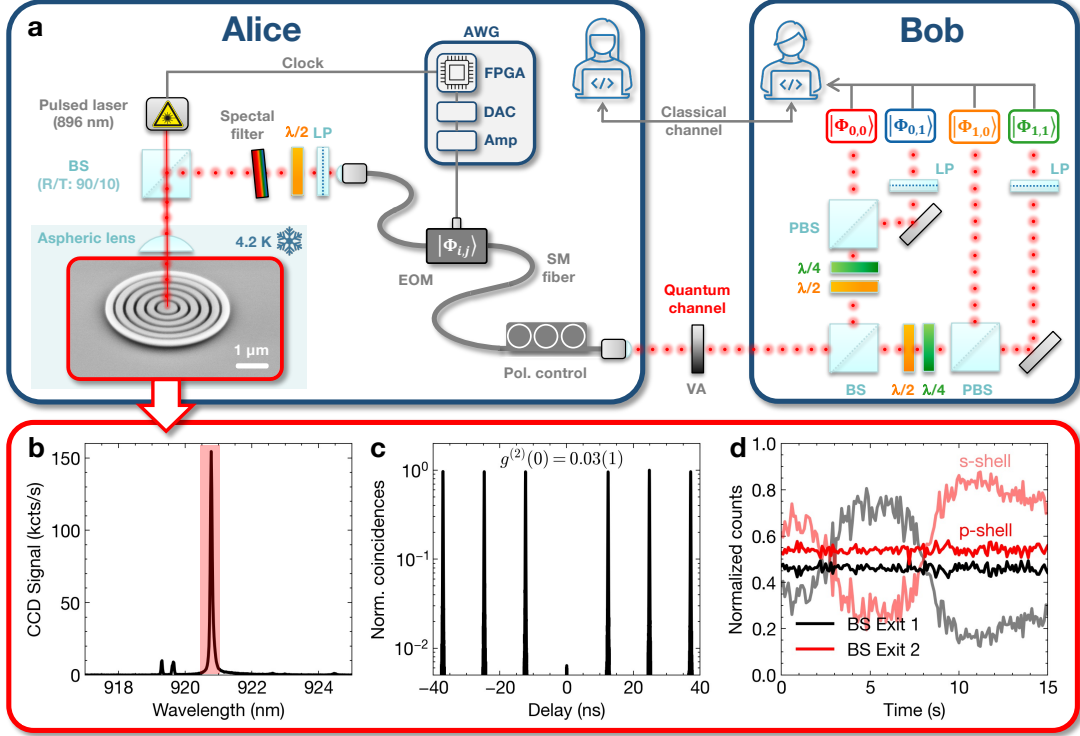


Figure 3. (a) Experimental setup for the implementation of QSCF: Alice generates single photons using an engineered single-photon source comprised of a single quantum dot deterministically integrated into a hybrid circular Bragg grating, and dynamically switches between the four QSCF states using a fiber-coupled electro-optical-modulator (EOM) controlled by a custom-built arbitrary waveform generator (AWG). The polarization-encoded qubits propagate through a quantum channel, including a variable attenuator for emulating loss. Bob uses a 4-state passive basis choice polarization analyzer to project the incoming single-photons into the four protocol states. Photons are detected using superconducting nanowire detectors in combination with time tagging electronics. (BS: beam splitter, LP: linear polarizer, PBS: polarizing beam splitter, DAC: digital-to-analog converter, FPGA: field-programmable-gate-array, Amp: Amplifier, EOM: electro-optical-modulator, SM: single-mode). (b) Emission spectrum of the single-photon source under quasi-resonant (p-shell) excitation revealing predominant emission of a trion transition (marked in red). (c) Hanbury-Brown and Twiss experiment confirming the single-photon nature of the spectrally filtered emission from (b). (d) Measurement of the photon number coherence (PNC) using phase-resolved two-photon interference experiments under p-shell (dark lines) and strict resonant (light lines) excitation. As QSCF requires vanishing PNC, quasi-resonant excitation was chosen for the protocol implementation in this work.

span a slightly larger voltage range.

Using the encoding system presented above, we experimentally achieve a QBER for dynamic random state switching of single-photon pulses of 2.8%. To our knowledge this is the smallest QBER reported so far for 80 MHz dynamic modulation of single-photon polarization states with a fiber-based EOM. Due to high extinction ratio polarizers in the detection module, the state discrimination does not increase the QBER as static state preparation yields QBER values below 0.1%.

D. Experimental quantum strong coin flipping

To implement the QSCF protocol, Alice randomly encodes the four protocol states for the fixed optimized value of $a = 0.9$ and a fixed number of repetitions $K = 50,000$. After the K

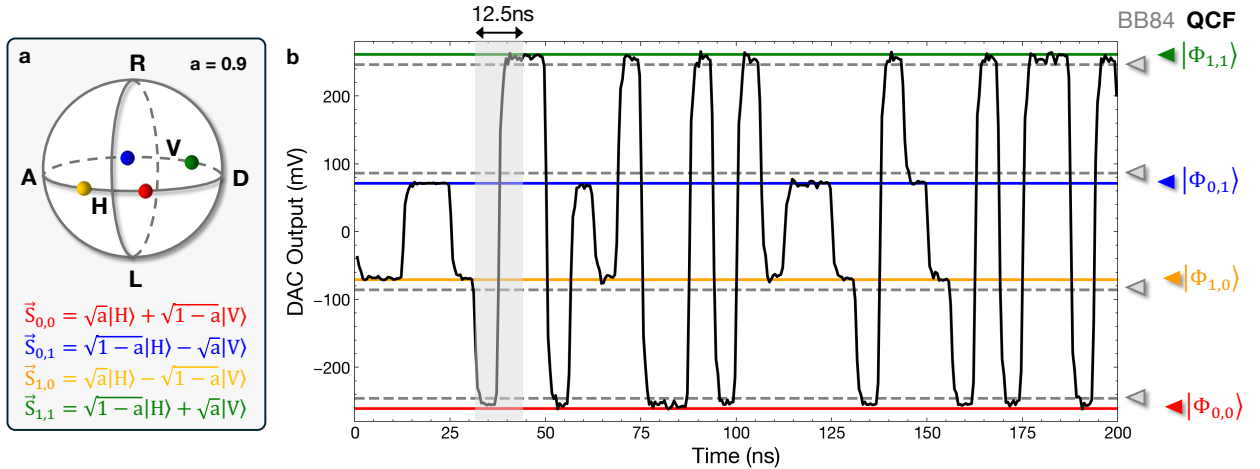


Figure 4. (a) The four states used in the QSCF protocol are defined by the parameter $a = 0.9$ and marked on the Poincaré sphere. (b) Exemplary sequence showing random voltage-level switching as used in our protocol implementation to modulate the EOM for dynamic polarization qubit encoding. Full horizontal lines indicate the four target states of the QSCF protocol. Dashed lines indicate the states typically used in BB84 QKD $\{H, D, V, A\}$ serving as a reference. Note that we employed an advanced coding scheme requiring an effectively doubled clock-rate of 160 MHz inside the control electronics preventing voltage level drifts as described in the main text. The gray shaded window indicates the 12.5 ns wide period defined by the 80 MHz laser clock-rate, where the polarization encoding of the photon is performed during the first 6.25 ns of the window.

voltage values, the sequence is repeated to evaluate the protocol performance with sufficient statistics. To realize the random bit sequence, we used a pre-stored set of quantum random numbers generated by measuring vacuum fluctuations [13, 28], which were provided by the Australian National University [14]. After propagation through the quantum channel, first in the back-to-back case without additional loss, Bob projects the arriving photons into the four protocol states by detecting them in his four detection channels yielding the arrival statistics shown for a short time period in Figure 5(a). Synchronizing the qubit-state preparation and detection using a trigger signal at the start of each protocol run, we are able to average over many realizations of the K -long random sequence. The relative temporal offset between Alice' and Bob's time-bins is determined by correlating a subset of the sequence for different relative shifts and channel permutations. This enables us to compare the detected state to the actually sent state for each time-bin (see Figure 5b), which yields a high extinction in the preparation basis and the expected projections in the other basis. Figure 5c presents the resulting input-output table that is expected from the a parameter (left panel) and for the experimental realizations with losses in the quantum channel of 0 dB (back-to-back), 3 dB, and 6 dB, resulting in a QBER of 2.8%, 3.1%, and 6.4% (right panels). The QBER obtained under dynamic random state preparation was calculated from the ratio of wrong projections divided by all projections for a given state and averaged over all four QSCF states. We observe a good agreement between the experimental performance and the theoretical expectations.

Performing the protocol steps outlined in section II A, coin flips are performed for each realization of the K -step long random sequence for the back-to-back case, yielding the performance summarized in Table II D. We perform 52,978 successful coin flips within 34s, yielding a rate of about 1,500 unbiased single-photon coin flips per second. Honest aborts due to sequences in which no photon is detected are almost negligible for the chosen length of K . Honest aborts due to deviations between Alice and Bob's outcomes, however, appear in $P_{AB} = 1.4\%$ of the cases, in good agreement with the theoretical prediction that the honest abort probability converges to QBER/2, as such an error is detected in 1/2 of the cases in the protocol. Using the a parameter and the photon statistics we can calculate the maximum cheating probabilities of Alice and Bob to be $P^A = P^B = 90.0\%$, confirming that the protocol is fair, while the coin flip outcome probabilities of $P_0 = 49.9\%$ and $P_1 = 50.1\%$ confirm the assumption of a random basis choice and the balanced generation of a random

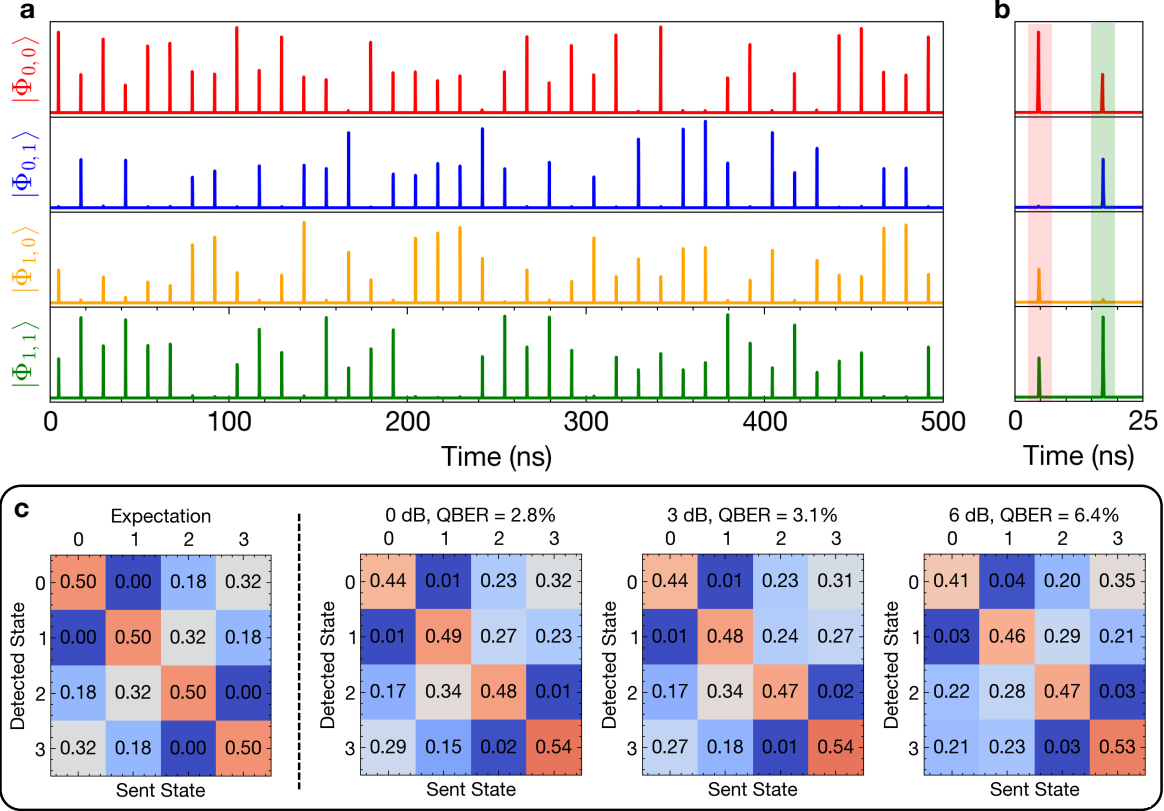


Figure 5. (a) Time traces of single-photon pulses under dynamic random switching between the four QSCF states as detected on Bob’s side after projection into the four different target channels (top to bottom). (b) Zoom-in from (a) with shaded regions indicating the prepared state by the color coding. (c) Integrating over all coin flip realizations and comparing prepared and detected states yields input-output tables from which the QBER can be computed. Introducing additional loss in the quantum channel, the QBER increases and the received statistics start to differ from the expected case for $a = 0.9$ (left panel).

bit. From the measured P_{AB} we can further estimate the equivalent cheating probability for a classical coin flipping protocol resulting in 91.6%. The smaller cheating probabilities observed for the quantum version of the coin flipping protocol demonstrates that we indeed experimentally achieved a quantum advantage. Moreover, the same protocol carried out with a phase-randomized WCP source of same μ using the same experimental setup would yield calculated cheating probabilities of 90.3%, higher than in the single-photon case. Hence, we demonstrate not only a quantum advantage, but also a single photon advantage compared to WCP-based implementations, as predicted in the protocol simulations.

	SPS Predicted	SPS Implemented	WCP Calculated	Classical Protocol
Honest abort prob. P_{AB}	1.4%	1.4%	1.4%	-
Bob cheating prob. P^B	90.0%	90.0%	90.3%	91.6%
Outcome '0' prob. P_0	50.0%	49.9%	-	-
Quantum Gain g	1.6%	1.6%	1.3%	-

Table II. Summary of QSCF protocol performance obtained from in back-to-back case (0 dB loss).

Next we investigate the performance of our QSCF implementation as a function of additional transmission loss of 3 dB and 6 dB in the free-space quantum channel, corresponding to several km of fiber-transmission representative for realistic urban quantum networks. To compensate for the decreasing number of photons detected in each K -long sequence with increasing transmission loss, we gradually increased K from $K = 25,000$ in the lossless case up to $K = 100,000$ for 6 dB attenuation. Figure 6a depicts the resulting honest abort probability $P_{A,B}$ as a function of the channel loss. We find that despite the gradual increase in K , the honest abort probability still increases due to the reduced signal-to-noise ratio causing an increased QBER. The increase in $P_{A,B}$ quantitatively matches the theoretical expectation (solid lines), as calculated from the experimentally measured QBER e and the selected length of the random sequence K .

The experimental quantum advantage achieved in our protocol implementation for the different channel attenuations is presented in Figure 6b, as calculated from the measured honest abort probabilities (points) together with the theoretically predicted honest abort probability (solid lines). We observe that a quantum advantage is maintained for 3 dB additional loss in the quantum channel, while no quantum advantage is currently possible at 6 dB loss due to the increased QBER. The experimental results are again in good agreement with the theoretical predictions. The decreasing quantum advantage with increasing loss thereby directly results from the increase of the honest abort probability, causing the classical cheating probability to decrease. The assumed maximum cheating probability in the QSCF protocol, on the other hand, does not depend on loss, as Bob could always replace the channel with a lossless one.

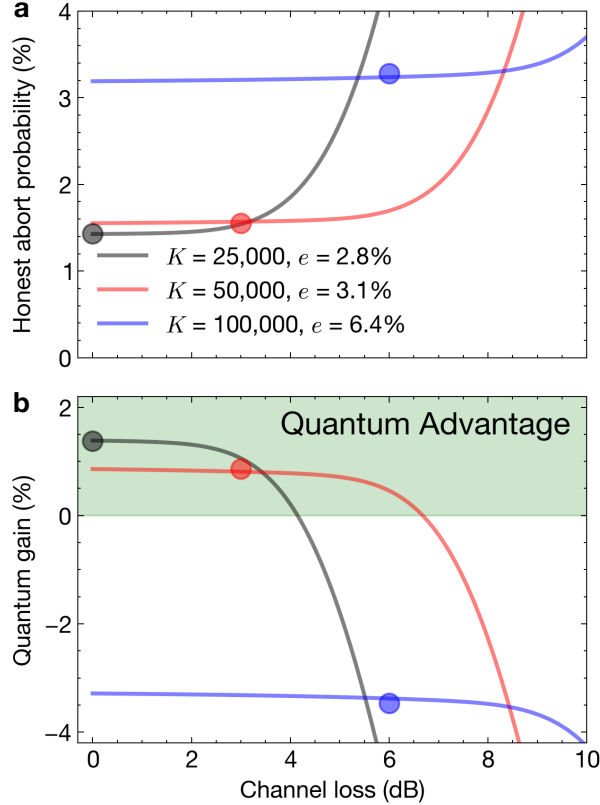


Figure 6. Performance of the QSCF implementation in the presence of additional loss in the quantum channel: (a) Experimentally determined honest abort probability due to no detections and wrong detections (points) match the theoretical expectation (solid lines) for the same K and QBER. (b) Quantum gain (difference between classical and quantum cheating probability) as calculated from the experimentally measured honest abort probabilities (points), shown together with the theoretical prediction (solid line). The green shaded region indicates a quantum advantage. In the high-loss regime the quantum gain vanishes due to the increasing QBER, which makes classical cheating more difficult. The length K of the single-photon sequence transmitted was gradually increased to compensate for the reduced number of detection events.

III. CONCLUSION AND OUTLOOK

In this work we have demonstrated, both theoretically and experimentally, that single-photon sources can be used to achieve a quantum advantage for essential cryptographic primitives beyond QKD. We implemented a QSCF protocol using a deterministic single-photon source based on a semiconductor quantum dot embedded in a high-Purcell photonic micro-cavity in combination with dynamic random polarization-state encoding with a

QBER of 2.8%. The implementation enabled us to experimentally achieve a single-photon advantage of up to 1.8% (1.6% percentage points) compared to a classical realization of the protocol. In addition we also verified a noticeable single-photon advantage compared to an implementation using faint laser pulses. The experimentally obtained performance is in good agreement with the theoretical predictions extracted from simulations. The observed single-photon advantage is a direct result of the sub-Poissonian photon statistics of the quantum light source used in our experiment. Moreover, we conducted QSCF experiments under variable attenuation inside the quantum channel, revealing that a quantum advantage can be maintained up to 3 dB of additional loss.

Our protocol implementation paves the way for further advancements in experimental QSCF in future work. Firstly, the QBER can be reduced further using a high-extinction ratio polarization-maintaining fiber at the EOM input. Moreover, pushing the clock-rate of our implementation from 80 MHz to the GHz-range, as readily possible with our current single-photon source [26], the quantum coin flipping rate can be increased by a factor $\times 16$ to 24,000 coin flips per second. This however will require a speed-up of the qubit-state encoder, currently limited to an electronic bandwidth of about 300 MHz. Furthermore, transferring our QSCF protocol implementation to telecom wavelength will significantly increase the possible communication distance in optical fibers. Finally, employing techniques for the direct fiber-pigtailing of deterministic quantum light sources [27] for the integration in compact cryocoolers, will enable the realization of bench-top server-rack compatible quantum coin flipping systems for field-experiments as previously demonstrated for QKD [11].

ACKNOWLEDGMENTS

The authors gratefully acknowledge early contributions to the experimental methodology and software by Timm Gao, experimental support by Bhavana Panchumathi, Aodhan Corrigan, and Calista Eitel-Porter, as well as technical support by Johannes Schall, Sven Rodt, Stephan Reitzenstein, and Chengao Yang. The authors further acknowledge financial support by the German Federal Ministry of Education and Research (BMBF) via the project “QuSecure” (Grant No. 13N14876) within the funding program Photonic Research Germany, the BMBF joint projects “tubLAN Q.0” (Grant No. 16KISQ087K) as well as QuNET+ICLink (Grant No. 16KIS1967) in the context of the federal government’s research

framework in IT-security “Digital. Secure. Sovereign.”, and the Einstein Foundation via the Einstein Research Unit “Quantum Devices”. A.P. also acknowledges financial support by the German Research Foundation (DFG) via the Emmy Noether (Grant No. 418294583). H.L., S.L., H.N., and Z.N. acknowledge financial support by the Chinese Academy of Sciences Project for Young Scientists in Basic Research (Grant No. YSBR-112) and National Natural Science Foundation of China (Grant No. 12494601).

AUTHOR CONTRIBUTION

D.A.V. and K.K. set up the quantum coin flipping experiment under supervision of M.v.H. and T.H.; F.D. and D.A.V. performed the protocol simulations. L.R. designed and fabricated the single-photon source based on the quantum dot wafer material provided/grown by H.L., S.L., H.N., and Z.N.; D.A.V., F.D., A.P., and T.H. prepared the paper with inputs from all authors; A.P. supervised the theoretical and T.H. the experimental aspects of the project; T.H. and A.P. jointly conceived the project.

-
- [1] D. Aharonov, A. Ta-Shma, U. V. Vazirani, and A. C. Yao. Quantum bit escrow. In *Proceedings of the Thirty-Second Annual ACM Symposium on Theory of Computing*, STOC '00, page 705–714, New York, NY, USA, 2000. Association for Computing Machinery.
- [2] C. H. Bennett and G. Brassard. Quantum Cryptography: Public key distribution and coin tossing. *Proceedings of IEEE International Conference on Computers, Systems and Signal Processing, Bangalore, India*, pages 175–179, 1984.
- [3] C. H. Bennett and G. Brassard. An update on quantum cryptography. In *Workshop on the theory and application of cryptographic techniques*, pages 475–480. Springer, 1984.
- [4] G. Berlín, G. Brassard, F. Bussières, and N. Godbout. Fair loss-tolerant quantum coin flipping. *Physical Review A*, 80(6):062321, 2009.
- [5] G. Berlín, G. Brassard, F. Bussières, N. Godbout, J. A. Slater, and W. Tittel. Experimental loss-tolerant quantum coin flipping. *Nature communications*, 2(1):1–7, 2011.
- [6] M. Blum. Coin flipping by telephone a protocol for solving impossible problems. *ACM SIGACT News*, 15(1):23–27, 1983.
- [7] M. Bozzio, U. Chabaud, I. Kerenidis, and E. Diamanti. Quantum weak coin flipping with a single photon. *Physical Review A*, 102(2):022414, 2020.
- [8] M. Bozzio, M. Vyvlecka, M. Cosacchi, C. Nawrath, T. Seidelmann, J. C. Loredó, S. L. Portalupi, V. M. Axt, P. Michler, and P. Walther. Enhancing quantum cryptography with quantum dot single-photon sources. *npj Quantum Information*, 8:1–8, 2022.
- [9] A. Broadbent and C. Schaffner. Quantum cryptography beyond quantum key distribution. *Designs, Codes and Cryptography*, 78:351–382, 2016.
- [10] R. Cleve. Limits on the security of coin flips when half the processors are faulty. In *Symposium on the Theory of Computing*, 1986.
- [11] T. Gao, L. Rickert, F. Urban, J. Große, N. Srocka, S. Rodt, A. Musiał, K. Żołnacz, P. Mergo, K. Dybka, et al. A quantum key distribution testbed using a plug&play telecom-wavelength single-photon source. *Applied Physics Reviews*, 9(1), 2022.
- [12] N. Gisin, G. Ribordy, W. Tittel, and H. Zbinden. Quantum cryptography. *Reviews of modern physics*, 74(1):145, 2002.

- [13] J.-Y. Haw, S. Assad, A. Lance, N. Ng, V. Sharma, P. K. Lam, and T. Symul. Maximization of extractable randomness in a quantum random-number generator. *Physical Review Applied*, 3(5):054004, 2015.
- [14] <https://qrng.anu.edu.au/>. accessed, August 13. 2024.
- [15] W.-Y. Hwang. Quantum key distribution with high loss: toward global secure communication. *Physical review letters*, 91(5):057901, 2003.
- [16] A. Y. Kitaev. Quantum coin flipping. *Lecture delivered at the 2003 Annual Quantum Information Processing (QIP) Workshop*, 2003.
- [17] H.-K. Lo and H. Chau. Why quantum bit commitment and ideal quantum coin tossing are impossible. *Physica D: Nonlinear Phenomena*, 120(1):177–187, 1998. Proceedings of the Fourth Workshop on Physics and Consumption.
- [18] D. Mayers. Unconditionally secure quantum bit commitment is impossible. *Phys. Rev. Lett.*, 78:3414–3417, Apr 1997.
- [19] C. Mochon. Quantum weak coin flipping with arbitrarily small bias. *arXiv preprint arXiv:0711.4114*, 2007.
- [20] G. Molina-Terriza, A. Vaziri, R. Ursin, and A. Zeilinger. Experimental quantum coin tossing. *Physical review letters*, 94(4):040501, 2005.
- [21] S. Neves, V. Yacoub, U. Chabaud, M. Bozzio, I. Kerenidis, and E. Diamanti. Experimental cheat-sensitive quantum weak coin flipping. *Nature Communications*, 14(1):1855, 2023.
- [22] A. T. Nguyen, J. Frison, K. P. Huy, and S. Massar. Experimental quantum tossing of a single coin. *New Journal of Physics*, 10(8):083037, 2008.
- [23] A. Pappa, A. Chailloux, E. Diamanti, and I. Kerenidis. Practical quantum coin flipping. *Physical Review A*, 84(5):052305, 2011.
- [24] A. Pappa, P. Jouguet, T. Lawson, A. Chailloux, M. Legré, P. Trinkler, I. Kerenidis, and E. Diamanti. Experimental plug and play quantum coin flipping. *Nature communications*, 5(1):1–8, 2014.
- [25] L. Rickert, T. Kupko, S. Rodt, S. Reitzenstein, and T. Heindel. Optimized designs for telecom-wavelength quantum light sources based on hybrid circular Bragg gratings. *Optics Express*, 27(25):36824, Dec. 2019.
- [26] L. Rickert, D. A. Vajner, M. von Helversen, J. Schall, S. Rodt, S. Reitzenstein, H. Liu, S. Li, H. Ni, Z. Niu, et al. High purcell-enhancement in quantum-dot hybrid circular bragg grating

- cavities for GHz-clockrate generation of indistinguishable photons. *ACS Photonics*, pages in–print, 2024.
- [27] L. Rickert, K. Żołnacz, D. A. Vajner, M. von Helversen, S. Rodt, S. Reitzenstein, H. Liu, S. Li, H. Ni, P. Wyborski, et al. A fiber-pigtailed quantum dot device generating indistinguishable photons at GHz clock-rates. *Nanophotonics*, pages in–print, 2024.
- [28] T. Symul, S. M. Assad, and P. K. Lam. Real time demonstration of high bitrate quantum random number generation with coherent laser light. *Applied Physics Letters*, 98(23), 2011.
- [29] E. Waks, A. Zeevi, and Y. Yamamoto. Security of quantum key distribution with entangled photons against individual attacks. *Physical Review A*, 65(5):052310, 2002.
- [30] S. Wiesner. Conjugate coding. *SIGACT News*, 15(1):78–88, jan 1983.